

# Conformal Invariance of the Transition Vertex

## $2 \rightarrow 4$ gluons

J. Bartels<sup>a</sup>, L.N.Lipatov<sup>b c 1</sup>, M.Wüsthoff<sup>a</sup>

<sup>a</sup>*II. Institut für Theoretische Physik, Universität Hamburg.*

<sup>b</sup>*Deutsches Elektronen Synchrotron, DESY, Hamburg.*

<sup>c</sup>*St.Petersburg Nuclear Physics Institute, 188350, Gatchina, Russia*

**Abstract:** We show that the transition vertex: two reggeized gluons  $\rightarrow$  four reggeized gluons is invariant under Möbius transformations. This provides an important step in defining a conformally invariant effective field theory for QCD in the Regge limit.

## 1 Introduction

The Balitsky-Fadin-Kuraev-Lipatov (BFKL) [1] Pomeron has recently attracted much interest, in particular in connection with the small- $x$  behavior of the deep inelastic structure function of the proton. The BFKL Pomeron represents, within QCD, the leading-logarithmic approximation of the Regge limit (energy  $s/Q^2 \approx 1/x_B \rightarrow \infty$ , momentum transfer  $t$  small and fixed). Since at large energies it violates the unitarity bound, there is no doubt that subleading corrections to the BFKL Pomeron are of vital importance, and strategies have to be found which allow the summation of all these contributions.

In [2, 3] it has been observed that the kernel of the BFKL Pomeron is invariant under Möbius transformations: in particular, starting from the Fourier transform of the BFKL equation, it has been shown that the equation remains invariant under the inversion  $\rho \rightarrow 1/\rho$  ( $\rho$  denotes the complex variable  $\rho_x + i\rho_y$  where  $\rho_x, \rho_y$  are the two components of the impact parameter). Moreover, when writing the BFKL evolution equation in the form of the Schroedinger equation, one can show that the Hamiltonian has the property of holomorphic separability, i.e. it can be written as a sum of two pieces which depend only upon  $\rho$  and  $\rho^*$ , resp. Both these properties can be derived most elegantly from the following representation of the Hamiltonian [3]:

$$\mathcal{H} = \frac{g^2 N_c}{8\pi^2} \left( \frac{1}{p_1 p_2^*} \ln |\rho_{12}|^2 p_1 p_2^* + \text{h.c.} + \ln |p_1|^2 + \ln |p_2|^2 - 4\psi(1) \right), \quad (1.1)$$

---

<sup>1</sup>Alexander von Humboldt Preisträger

where  $p_r = i \frac{\partial}{\partial \rho_r}$ . This Hamiltonian can be split into two pieces:

$$\mathcal{H} = H + H^* \quad (1.2)$$

with

$$H = \frac{g^2 N_c}{8\pi^2} \left( \frac{1}{p_1} \ln \rho_{12} p_1 + \frac{1}{p_2} \ln \rho_{12} p_2 + \ln(p_1 p_2) - 2\psi(1) \right). \quad (1.3)$$

After some algebra one finds that (1.3) is identical with:

$$H = \frac{g^2 N_c}{8\pi^2} \left( \ln(\rho_{12}^2 p_1) + \ln(\rho_{12}^2 p_2) - 2 \ln \rho_{12} - 2\psi(1) \right). \quad (1.4)$$

(both representations (1.3) and (1.4) are, strictly speaking, somewhat symbolic as long as one does not specify the boundary conditions for the integral operators).

Eq.(1.2) means that the Hamiltonian has the property of holomorphic separability, and the invariance under Möbius transformations (in particular the inversion  $\rho \rightarrow 1/\rho$ ) can be deduced from (1.4). The importance of these properties is rather obvious: the separability reduces the two-dimensional problem to a one-dimensional one (instead of quantum mechanics in a plane one is dealing with quantum mechanics on a line), and the symmetry allows to solve the eigenvalue problem in terms of the representations of the Möbius group. In this way it was possible to solve the BFKL equation also in the nonforward direction.

As far as the restoration of unitarity is concerned it is believed that the most important corrections will come from diagrams with a large number of (reggeized) gluons in the t-channel. As a first step, one considers diagrams [4] where  $n$ , the number of gluons in the t-channel, is conserved. The high energy behavior of these contributions is given by the energy spectrum of a quantum mechanical system of  $n$  particles with pairwise interactions through the BFKL kernel. As a result of the conformal symmetry of the BFKL Hamiltonian (1.1) - (1.4), it is tempting to expect that the problem of determining the energy spectrum may be exactly soluble: in fact, for the large- $N_c$  limit it has been shown [5, 6] that the system is equivalent to the XXX Heisenberg model for spin zero, and the energy behaviour can, at least in principle, be computed analytically.

As the next step in this direction, one has to adress the question whether there are kernels which change the number of t-channel gluons. For the simplest case, the transition from 2 to 4 gluons, a new kernel has been derived in [7, 8], which, similar to the BFKL kernel, consists of several pieces. The fact that such a number-changing vertex exists means that the quantum mechanical problem ("no particle production") studied in [5, 6], in fact, will turn into a quantum field theory in 2+1 dimensions. In view of the conformal symmetry which, in the case of the  $n$ -gluon system, has turned out to be so powerful, we are then facing the question whether the same symmetry is preserved also by the new transition vertex. If so, there is hope that even the field theory may have an analytic solution. It is the purpose of this paper to show that, in fact, the new transition vertex is invariant under conformal (Möbius) transformations.

To complete this short overview of strategies beyond the BFKL approximation, it is important to note that both the BFKL kernel (which contains, as a part of it, also the gluon trajectory function) and the transition vertex have so far been computed only in leading order of  $\alpha_s$ . For the BFKL kernel, calculations of the  $\alpha_s^2$  corrections are partly been done [9]. Interest in these corrections also comes from the recent observation [10, 11, 12] that a resummation of the singular

terms in the quark and gluon anomalous dimension seems to play a very crucial role in the GLAP evolution at small  $x$ . A field theoretic formulation (effective action) which takes into account these nonleading corrections to all orders has recently been suggested in [13, 14].

This paper is organized as follows. Since the transition vertex cannot be brought into a compact form analogous to (1.1) which would allow to derive both symmetry and separability in a rather elegant and straightforward fashion, we first (section 2) review the explicit proof of conformal invariance of the BFKL kernel. We then (section 3) define the transition vertex for  $2 \rightarrow 4$  gluons and present a brief sketch of its derivation. The proof of the conformal invariance is contained in section 4, and in section 5 we conclude with a brief summary.

## 2 Conformal Invariance of the BFKL Kernel

### 2.1 Fourier Transform of the BFKL Kernel

In this section we briefly repeat, as an illustration and as a preparatory step, the proof of conformal invariance of the BFKL kernel (Fig.1). The (non-amputated) amplitude will be denoted by  $\Phi_2(q_1, q_2)$  (we suppress the dependence upon angular momentum  $\omega$ ). We first discuss the Fourier transform and then prove the invariance under the inversion  $\rho \rightarrow 1/\rho$ .

It will be convenient to introduce complex coordinates in the two-dimensional transverse space:

$$\mathbf{q} = (q_x, q_y) \quad (2.1)$$

$$q = q_x + iq_y, \quad q^* = q_x - iq_y \quad (2.2)$$

$$\mathbf{q} \cdot \boldsymbol{\rho} = \frac{1}{2}(q\rho^* + q^*\rho). \quad (2.3)$$

The gluon production vertex then reads (in the light-cone gauge of [14])

$$\mathcal{C}_1 = -2q_1 q_{1'}^* \frac{1}{(q_{1'} - q_1)^*}, \quad (2.4)$$

and for the squared production amplitude one obtains

$$\mathcal{C}_\mu \mathcal{C}^\mu = \frac{q_1 q_{1'}^* q_2 q_2^*}{(\mathbf{q}_{1'} - \mathbf{q}_1)^2} + \text{h.c.} \quad (2.5)$$

After multiplication with the inverse propagators for the upper gluons the integral in Fig.1 takes the well-known form:

$$\begin{aligned} |q_1|^2 |q_2|^2 (\mathcal{K} \Phi_2)(\mathbf{q}_1, \mathbf{q}_2) &= \int d^2 \mathbf{q}_{1'} \left( \frac{q_1 q_{1'}^* q_2 q_2^*}{|q_{1'} - q_1|^2 + \lambda^2} + \text{h.c.} \right) \Phi_2(\mathbf{q}_{1'}, \mathbf{q}_{2'}) \\ &\quad - \pi \left( \ln \frac{|q_1|^2}{\lambda^2} + \ln \frac{|q_2|^2}{\lambda^2} \right) |q_1|^2 |q_2|^2 \Phi_2(\mathbf{q}_1, \mathbf{q}_2). \end{aligned} \quad (2.6)$$

Here we have introduced the infrared regulator  $\lambda^2$  (gluon mass), which later on we shall remove again. Assuming that  $\Phi_2$  is invariant under Möbius transformations, we shall prove that the integral on the rhs remains invariant.

The Fourier transformation is defined as follows

$$\Phi_2(\boldsymbol{\rho}_1, \boldsymbol{\rho}_2) = \int \frac{d^2 \mathbf{q}_1 d^2 \mathbf{q}_2}{(2\pi)^4} \exp [i \mathbf{q}_1 \boldsymbol{\rho}_1 + i \mathbf{q}_2 \boldsymbol{\rho}_2] \Phi_2(\mathbf{q}_1, \mathbf{q}_2), \quad (2.7)$$

and we begin with the gluon trajectory function. Inserting

$$1 = \frac{1}{(2\pi)^2} \int d^2 \boldsymbol{\rho}_0 \int d^2 \mathbf{k} e^{i \boldsymbol{\rho}_0 (\mathbf{k} - \mathbf{q}_1)} \quad (2.8)$$

we obtain

$$- \Delta_1 \Delta_2 \int d^2 \boldsymbol{\rho}_0 \left[ \frac{1}{(2\pi)^2} \int d^2 \mathbf{k} e^{i \mathbf{k} (\boldsymbol{\rho}_1 - \boldsymbol{\rho}_0)} \pi \ln \frac{|k|^2}{\lambda^2} \right] \Phi_2(\boldsymbol{\rho}_0, \boldsymbol{\rho}_2). \quad (2.9)$$

For the integral in brackets we introduce the ultraviolet cutoff parameter  $\epsilon$  which will be removed at the end of our calculations:

$$- \left[ \frac{1}{(2\pi)^2} \int d^2 \mathbf{k} e^{i \mathbf{k} (\boldsymbol{\rho}_1 - \boldsymbol{\rho}_0)} \pi \ln \frac{|k|^2}{\lambda^2} \right] = \Gamma(\boldsymbol{\rho}_1 - \boldsymbol{\rho}_0) \quad (2.10)$$

$$\Gamma(\boldsymbol{\rho}_1 - \boldsymbol{\rho}_0) = \frac{1}{|\boldsymbol{\rho}_{10}|^2} \theta(|\boldsymbol{\rho}_{10}| - \epsilon) + c(\epsilon, \lambda) \delta^{(2)}(\boldsymbol{\rho}_{10}). \quad (2.11)$$

The function  $c(\epsilon, \lambda)$  is obtained from the integral

$$\begin{aligned} \int d^2 \boldsymbol{\rho} \frac{1}{|\boldsymbol{\rho}|^2} \theta(|\boldsymbol{\rho}| - \epsilon) e^{-i \mathbf{k} \boldsymbol{\rho}} &= \int_0^{2\pi} d\varphi \int_\epsilon^\infty \frac{d|\boldsymbol{\rho}|}{|\boldsymbol{\rho}|} \exp(-i|k||\boldsymbol{\rho}| \cos \varphi) \\ &= 2\pi [\psi(1) - \ln(\epsilon|k|)] - 4 \int_0^{\pi/2} d\varphi \ln(\cos \varphi) + O(\epsilon) \\ &= 2\pi \left[ \psi(1) + \ln \frac{2}{\epsilon|k|} \right] + O(\epsilon), \end{aligned} \quad (2.12)$$

where the series representation of the Exponential-integral has been used neglecting the terms proportional to  $\epsilon$ . We then find for  $c(\epsilon, \lambda)$ :

$$c(\epsilon, \lambda) = 2\pi [\ln \lambda + \ln \frac{\epsilon}{2} - \psi(1)]. \quad (2.13)$$

Next we turn to the Fourier transform of the first term on the rhs of eq.(2.6), the square of the production vertex. We make use of the complex coordinates, defined in eqs.(2.1) - (2.3). With  $\partial = \partial/\partial \rho$ ,  $\partial^* = \partial/\partial \rho^*$ ,  $\Delta = 4\partial\partial^*$  we find:

$$\begin{aligned} & \int \frac{d^2 \mathbf{q}_1 d^2 \mathbf{q}_2}{(2\pi)^4} e^{i \mathbf{q}_1 \boldsymbol{\rho}_1 + i \mathbf{q}_2 \boldsymbol{\rho}_2} \int d^2 \mathbf{q}_{1'} \left( \frac{q_1 q_{1'}^* q_2 q_2^*}{|q_{1'} - q_1|^2 + \lambda^2} + \text{h.c.} \right) \Phi_2(\mathbf{q}_{1'}, \mathbf{q}_{2'}) \\ &= \int d^2 \boldsymbol{\rho}_1 d^2 \boldsymbol{\rho}_{2'} \int \frac{d^2 \mathbf{q}_1 d^2 \mathbf{q}_2}{(2\pi)^4} d^2 \mathbf{k} \frac{16}{|k|^2 + \lambda^2} \partial_1^* \partial_2 e^{-i \mathbf{k} (\boldsymbol{\rho}_{1'} - \boldsymbol{\rho}_{2'})} \cdot \\ & \quad \cdot e^{i \mathbf{q}_1 (\boldsymbol{\rho}_1 - \boldsymbol{\rho}_{1'}) + i \mathbf{q}_2 (\boldsymbol{\rho}_2 - \boldsymbol{\rho}_{2'})} \partial_{1'} \partial_2^* \Phi_2(\boldsymbol{\rho}_{1'}, \boldsymbol{\rho}_{2'}) + \text{h.c.} \\ &= 16 \left( \partial_1^* \partial_2 \int d^2 \mathbf{k} \frac{1}{|k|^2 + \lambda^2} e^{-i \mathbf{k} (\boldsymbol{\rho}_1 - \boldsymbol{\rho}_2)} \partial_1 \partial_2^* + \text{h.c.} \right) \Phi_2(\boldsymbol{\rho}_1, \boldsymbol{\rho}_2). \end{aligned} \quad (2.14)$$

The  $\mathbf{k}$  - integral gives

$$2\pi[\ln \frac{2}{|\boldsymbol{\rho}_{12}|} - \ln \lambda + \psi(1)], \quad (2.15)$$

where we have used the integral:

$$\begin{aligned} \int d^2\mathbf{k} \frac{e^{i\mathbf{k}\boldsymbol{\rho}}}{\mathbf{k}^2 + \lambda^2} &= \int_0^{2\pi} d\varphi \int_0^\infty d|k| \frac{|k| \exp(i|k||\boldsymbol{\rho}| \cos \varphi)}{|k|^2 + \lambda^2} \\ &= \frac{1}{2} \int_0^{2\pi} d\varphi \int_0^\infty d|k| \exp(i|k||\boldsymbol{\rho}| \cos \varphi) \left( \frac{1}{|k| + i\lambda} + \frac{1}{|k| - i\lambda} \right) \\ &= 2\pi \left[ \psi(1) + \ln \frac{2}{|\boldsymbol{\rho}|\lambda} \right] + O(\lambda) . \end{aligned} \quad (2.16)$$

Moving from the second to the third line in eq.(2.16) we have shifted the integration variable  $|k|$  by  $-i\lambda$  in the first and  $+i\lambda$  in the second term. After that the series representation of the Exponential-integral similarly to eq.(2.12) was used. Comparing with eq.(2.9)-(2.13) we find that  $\psi(1) - \ln \lambda + \ln 2$  cancels between the trajectory and the production vertex, and our eq.(2.6) in configuration space reads <sup>2</sup>:

$$\begin{aligned} |\partial_1|^2 |\partial_2|^2 (\mathcal{K}\Phi)(\boldsymbol{\rho}_1, \boldsymbol{\rho}_2) &= |\partial_1|^2 |\partial_2|^2 \int \frac{d^2\boldsymbol{\rho}_0}{|\boldsymbol{\rho}_{10}|^2} \theta(|\boldsymbol{\rho}_{10}| - \epsilon) \Phi_2(\boldsymbol{\rho}_0, \boldsymbol{\rho}_2) \\ &+ |\partial_1|^2 |\partial_2|^2 \int \frac{d^2\boldsymbol{\rho}_0}{|\boldsymbol{\rho}_{20}|^2} \theta(|\boldsymbol{\rho}_{20}| - \epsilon) \Phi_2(\boldsymbol{\rho}_1, \boldsymbol{\rho}_0) \\ &+ 4\pi \ln \epsilon |\partial_1|^2 |\partial_2|^2 \Phi_2(\boldsymbol{\rho}_1, \boldsymbol{\rho}_2) - [2\pi \partial_1^* \partial_2 \ln |\boldsymbol{\rho}_{12}| \partial_1 \partial_2^* + \text{h.c.}] \Phi_2(\boldsymbol{\rho}_1, \boldsymbol{\rho}_2). \end{aligned} \quad (2.17)$$

We still rearrange the differential operators in the first two terms, using partial integration

$$\begin{aligned} \partial_1 \partial_1^* \int d^2\boldsymbol{\rho}_0 g(|\boldsymbol{\rho}_{10}|^2) \Phi_2(\boldsymbol{\rho}_0, \boldsymbol{\rho}_2) &= \partial_1 \int d^2\boldsymbol{\rho}_0 \partial_1^* g(\rho_{10} \rho_{10}^*) \Phi_2(\boldsymbol{\rho}_0, \boldsymbol{\rho}_2) \\ &= \partial_1 \int d^2\boldsymbol{\rho}_0 (-1) \partial_0^* g(\rho_{10} \rho_{10}^*) \Phi_2(\boldsymbol{\rho}_0, \boldsymbol{\rho}_2) = \partial_1 \int d^2\boldsymbol{\rho}_0 g(|\boldsymbol{\rho}_{10}|^2) \partial_0^* \Phi_2(\boldsymbol{\rho}_0, \boldsymbol{\rho}_2). \end{aligned} \quad (2.18)$$

Distributing the derivatives in a symmetric way we end up with

$$\begin{aligned} 2 |\partial_1|^2 |\partial_2|^2 (\mathcal{K}\Phi)(\boldsymbol{\rho}_1, \boldsymbol{\rho}_2) &= \partial_1 \partial_2^* \int \frac{d^2\boldsymbol{\rho}_0}{|\boldsymbol{\rho}_{10}|^2} \theta(|\boldsymbol{\rho}_{10}| - \epsilon) \partial_0^* \partial_2 \Phi_2(\boldsymbol{\rho}_0, \boldsymbol{\rho}_2) \\ &- 2\pi \partial_1 \partial_2^* \ln |\boldsymbol{\rho}_{12}| \partial_1^* \partial_2 + 2\pi \ln \epsilon |\partial_1|^2 |\partial_2|^2 \Phi_2(\boldsymbol{\rho}_1, \boldsymbol{\rho}_2) + \text{h.c.} + [1 \leftrightarrow 2]. \end{aligned} \quad (2.19)$$

Due to the logarithmic divergence at  $\boldsymbol{\rho}_0 = \boldsymbol{\rho}_1$  any change of the argument of the  $\theta$ -function has to be compensated by an appropriate logarithmic term. In the case of eq.(2.19) the following equality applies:

$$\int \frac{d^2\boldsymbol{\rho}_0}{|\boldsymbol{\rho}_{10}|^2} \theta(|\boldsymbol{\rho}_{10}| - \epsilon) f(\boldsymbol{\rho}_0) = \int \frac{d^2\boldsymbol{\rho}_0}{|\boldsymbol{\rho}_{10}|^2} \theta\left(\frac{|\boldsymbol{\rho}_{10}|}{|\boldsymbol{\rho}_{12}|} - \epsilon\right) f(\boldsymbol{\rho}_0) + 2\pi \ln |\boldsymbol{\rho}_{12}| f(\boldsymbol{\rho}_1), \quad (2.20)$$

where  $f(\boldsymbol{\rho}_0)$  denotes the remainder of the integrand in (2.19) which is regular near  $\boldsymbol{\rho}_0 = \boldsymbol{\rho}_1$ . The kernel finally achieves the form <sup>3</sup>:

$$\begin{aligned} 2 |\partial_1|^2 |\partial_2|^2 (\mathcal{K}\Phi)(\boldsymbol{\rho}_1, \boldsymbol{\rho}_2) &= \partial_1 \partial_2^* \int \frac{d^2\boldsymbol{\rho}_0}{|\boldsymbol{\rho}_{10}|^2} \theta\left(\frac{|\boldsymbol{\rho}_{10}|}{|\boldsymbol{\rho}_{12}|} - \epsilon\right) \partial_0^* \partial_2 \Phi_2(\boldsymbol{\rho}_0, \boldsymbol{\rho}_2) \\ &+ 2\pi \ln \epsilon |\partial_1|^2 |\partial_2|^2 \Phi_2(\boldsymbol{\rho}_1, \boldsymbol{\rho}_2) + \text{h.c.} + [1 \leftrightarrow 2]. \end{aligned} \quad (2.21)$$

<sup>2</sup>We have taken out a factor 16 on both sides

<sup>3</sup>This form has first been used in [15] for the Odderon problem in QCD.

## 2.2 Invariance under Inversion

Now we want to verify that the configuration space kernel is invariant under conformal transformations. It is rather obvious that the kernel in (2.21) is invariant under dilatations, translations and rotations. The only property to be shown is the invariance under inversions. Let us perform the transformation

$$\rho_i \rightarrow \frac{1}{\rho_i} \quad (2.22)$$

$$\partial_i \rightarrow -\rho_i^2 \partial_i \quad (2.23)$$

$$d^2 \rho_0 \rightarrow \frac{d^2 \rho_0}{|\rho_0|^4} \quad (2.24)$$

$$|\rho_{i0}|^2 \rightarrow \frac{|\rho_{i0}|^2}{|\rho_i|^2 |\rho_0|^2} \quad (2.25)$$

and apply this transformation to the integral kernel. We obtain

$$\begin{aligned} & 2 |\rho_1|^4 |\rho_2|^4 |\partial_1|^2 |\partial_2|^2 (\mathcal{K}\Phi)(\boldsymbol{\rho}_1, \boldsymbol{\rho}_2) \\ &= \rho_1^2 \rho_2^{*2} \partial_1 \partial_2^* \int \frac{d^2 \boldsymbol{\rho}_0}{|\rho_{10}|^2} \frac{|\rho_1|^2 |\rho_0|^2}{|\rho_0|^4} \theta\left(\frac{|\rho_{10}| |\rho_2|}{|\rho_{12}| |\rho_0|} - \epsilon\right) \rho_0^{*2} \rho_2^2 \partial_0^* \partial_2 \Phi_2(\boldsymbol{\rho}_0, \boldsymbol{\rho}_2) \\ &\quad + 2\pi \ln \epsilon |\partial_1|^2 |\partial_2|^2 \Phi_2(\boldsymbol{\rho}_1, \boldsymbol{\rho}_2) + \text{h.c.} + [1 \leftrightarrow 2] \\ &= |\rho_1|^4 |\rho_2|^4 \partial_1 \partial_2^* \int \frac{d^2 \boldsymbol{\rho}_0}{|\rho_{10}|^2} \frac{\rho_0^* \rho_1}{\rho_1^* \rho_0} \theta\left(\frac{|\rho_{10}| |\rho_2|}{|\rho_{12}| |\rho_0|} - \epsilon\right) \partial_0^* \partial_2 \Phi_2(\boldsymbol{\rho}_0, \boldsymbol{\rho}_2) \\ &\quad + 2\pi \ln \epsilon |\partial_1|^2 |\partial_2|^2 \Phi_2(\boldsymbol{\rho}_1, \boldsymbol{\rho}_2) + [\text{h.c.}] + [1 \leftrightarrow 2]. \end{aligned} \quad (2.26)$$

We rewrite the numerator in front of the  $\theta$  - function as

$$\begin{aligned} \rho_0^* \rho_1 &= (\rho_{01}^* + \rho_1^*)(\rho_{10} + \rho_0) \\ &= \rho_{01}^* \rho_{10} + \rho_{01}^* \rho_0 + \rho_1^* \rho_{10} + \rho_1^* \rho_0 \end{aligned} \quad (2.27)$$

and consider the four terms separately. For the first three terms the singularity in  $\boldsymbol{\rho}_0 = \boldsymbol{\rho}_1$  becomes integrable and the  $\theta$  - function can be removed. We obtain for the first term:

$$|\rho_1|^4 |\rho_2|^4 \partial_1 \partial_2^* \int d^2 \boldsymbol{\rho}_0 \frac{-1}{\rho_1^* \rho_0} \partial_0^* \partial_2 \Phi_2(\boldsymbol{\rho}_0, \boldsymbol{\rho}_2) = |\rho_1|^4 |\rho_2|^4 \pi \delta^{(2)}(\boldsymbol{\rho}_1) |\partial_2|^2 \Phi_2(0, \boldsymbol{\rho}_2), \quad (2.28)$$

where the rhs emerges after partial integration with respect to  $\boldsymbol{\rho}_0$  and the use of the following identities

$$\Delta \ln |\boldsymbol{\rho}|^2 = 4 \partial \partial^* \ln |\boldsymbol{\rho}|^2 = 4\pi \delta^{(2)}(\boldsymbol{\rho}) \quad (2.29)$$

$$\partial \frac{1}{\rho^*} = \partial^* \frac{1}{\rho} = \pi \delta^{(2)}(\boldsymbol{\rho}) . \quad (2.30)$$

The second and third term of (2.28) are calculated in a similar way:

$$\begin{aligned} & |\rho_1|^4 |\rho_2|^4 \partial_1 \partial_2^* \int d^2 \boldsymbol{\rho}_0 \left[ \frac{1}{\rho_1^* \rho_{01}} + \frac{1}{\rho_0 \rho_{10}^*} \right] \partial_0^* \partial_2 \Phi_2(\boldsymbol{\rho}_0, \boldsymbol{\rho}_2) \\ &= |\rho_1|^4 |\rho_2|^4 \left[ -\partial_1 \frac{1}{\rho_1^*} + \frac{1}{\rho_1} \partial_1^* \right] |\partial_2|^2 \Phi_2(\boldsymbol{\rho}_1, \boldsymbol{\rho}_2) . \end{aligned} \quad (2.31)$$

The conjugate expression gives

$$|\rho_1|^4 |\rho_2|^4 \left[ -\partial_1^* \frac{1}{\rho_1} + \frac{1}{\rho_1^*} \partial_1 \right] |\partial_2|^2 \Phi_2(\rho_1, \rho_2). \quad (2.32)$$

After commutation of derivatives we obtain terms proportional to  $\delta^{(2)}(\rho_1)$  - functions which cancel against (2.28); the remaining terms in (2.31) and (2.32) add up to zero. Consequently the only contribution comes from the fourth term of (2.27), i.e. after the transformation (2.22) the kernel (2.21) reads

$$\begin{aligned} 2 |\rho_1|^4 |\rho_2|^4 |\partial_1|^2 |\partial_2|^2 (\mathcal{K}\Phi)(\rho_1, \rho_2) &= |\rho_1|^4 |\rho_2|^4 \rho_1^2 \rho_2^{*2} \partial_1 \partial_2^* \int \frac{d^2 \rho_0}{|\rho_{10}|^2} \theta\left(\frac{|\rho_{10}| |\rho_2|}{|\rho_{12}| |\rho_0|} - \epsilon\right) \partial_0^* \partial_2 \Phi_2(\rho_0, \rho_2) \\ &\quad + 2\pi \ln \epsilon |\partial_1|^2 |\partial_2|^2 \Phi_2(\rho_1, \rho_2) + [\text{h.c.}] + [1 \leftrightarrow 2]. \end{aligned} \quad (2.33)$$

By changing the argument of the  $\theta$  - function analogous to eq.(2.20) the factor  $|\rho_2|/|\rho_0|$  in the argument is eliminated. The extra term  $\ln(|\rho_2|/|\rho_1|)$  which arises after the change of the argument cancels due to its antisymmetry under  $1 \leftrightarrow 2$ . After removing the overall factor  $|\rho_1|^4 |\rho_2|^4$ , we recover the original expression (2.21).

### 3 The Transition Vertex

Before we start investigating the symmetry properties of the transition vertex [8] we present a brief qualitative discussion of how this vertex is derived; in particular we would like to emphasize that the derivation of this vertex cannot be understood without the reggeization of the gluon.

Let us first go back to the BFKL kernel. In the previous section we have already made use of the fact that it is derived from an effective production vertex (Fig.2a): an s-channel gluon is produced from a reggeized t-channel gluon, and the “square” of this production vertex leads to the (connected) part of the BFKL kernel. The iteration of this kernel in the t-channel defines the BFKL Pomeron, where the t-channel gluons are reggeized. It is then often convenient to rearrange the sum of ladders by combining the trajectory function of the t-channel gluons with the BFKL kernel. This gives rise to the additional (disconnected) piece in the kernel (Fig.2b) which serves as a regulator in the infrared region, and the t-channel gluons now come with ordinary propagators  $1/k^2$ . A similar structure has been found for the  $2 \rightarrow 4$  transition vertex. The basic (connected) contribution is obtained by taking products of higher order production vertices (Fig.3a). Disconnected pieces appear if we include other production mechanisms (an example is given in Fig.3b) and make use of the fact that, in the three gluon amplitude above the s-channel gluon, there is a contribution <sup>4</sup> where the two gluon lines on the right reggeize into a single gluon (Fig.3c). By applying this type of arguments to all possible production vertices and invoking reggeization for the three gluon amplitude above, one arrives at a  $2 \rightarrow 4$  transition vertex which consists of connected and disconnected pieces, in close analogy with the BFKL kernel.

However, this is not yet the final form of the vertex. The four gluon amplitude obtained so far still includes the possibility that the gluons at the bottom may reggeize, e.g. the two gluons on the left

---

<sup>4</sup>As it is shown in [7], the three gluon amplitude can be written as a sum of three terms, corresponding to the reggeization of gluon pairs (12), (23), (13), respectively.

and the two gluons on the right may form a single gluon each. It turns out that contributions of this kind have to be *subtracted* from the previous four gluon amplitude, and only the remainder defines the final  $2 \rightarrow 4$  transition vertex.

Let us then state the form of the transition vertex which we are going to use. Following [8] we write

$$V^{a_1, a_2, a_3, a_4}(k_1, k_2, k_3, k_4) = \delta^{a_1, a_2} \delta^{a_3, a_4} V(k_1, k_2, k_3, k_4) \\ + \delta^{a_1, a_3} \delta^{a_2, a_4} V(k_1, k_3, k_2, k_4) + \delta^{a_1, a_4} \delta^{a_2, a_3} V(k_1, k_4, k_2, k_3), \quad (3.1)$$

where the  $\delta$ -symbols refer to the color structure, and the momentum space expressions for the function  $V(k_1, k_2, k_3, k_4)$  can be found in [8] and will not be presented here. Instead we make use of the graphical representation shown in Fig.4 and adopt the following rules:

- (1) each line with (transverse) momentum  $k$  has a propagator  $1/k^2$ , each closed loop the integral  $\int \frac{d^2 k}{(2\pi)^3}$ .
- (2) each vertex carries a factor  $q^2$  where  $q$  denotes the sum of momenta above or below the vertex.
- (3) Sum over the permutations of external momenta, as indicated in Fig.4.
- (4) at the end, multiply with the overall factor  $\frac{g^4}{4\sqrt{2}}$ .

In the following section we shall show that this function  $V$  is invariant under (conformal) Möbius transformations.

It should be remarked that the diagrams in Fig.4 may also be grouped in a different way allowing the use of the complex notation for the effective emission vertex (or Lipatov vertex). In particular, when addressing the question of holomorphic separability the complex notation is needed and hopefully leads to an operator like approach similar to that found for the BFKL-kernel in eqs.(1.1)-(1.4). For the purpose of this paper, the proof of the conformal invariance of  $V$ , the representation in Fig.4 turned out to be more convenient. questions concerning the holomorphic separability will be discussed elsewhere.

## 4 Proof of the conformal invariance

Let us first define the expression which we are going to investigate (Fig.5): the upper blob denotes the two-gluon amplitude  $\Phi_2$  of the previous section which includes the  $1/k^2$  propagators of the upper two internal gluon lines. Correspondingly, we absorb the propagators of the four lower internal lines into the lower blob which we denote by  $\Phi_4(k_1, k_2, k_3, k_4)$  (we again suppress the  $\omega$ -dependence). Fourier transforms are defined as in (2.7). We shall make use of the fact [2, 3] that  $\Phi_2$  and  $\Phi_4$  have already been shown to be invariant under conformal transformations, and we prove that the additional integral which involves the new transition kernel preserves this symmetry, in particular the invariance with respect to the inversion.

We divide the set of graphs shown in Fig.4 into the four groups A, B, C, D. The last group D is easily recognized as the BFKL kernel, with the lower momenta being  $k_1 + k_2$  and  $k_3 + k_4$ . The conformal invariance of this expression has been proven in the previous section. For the other three groups we will proceed in the same fashion as in section 2: starting from the momentum space expressions of Fig.4 we first derive the representations in configuration space and then prove the invariance under inversion. We shall find that none of the subsets A, B, C is invariant by itself; only the the sum of all terms has the symmetry property.

Let us begin with the group C and consider the first line with the momenta (1234). It consists of three pieces which in configuration space take the form (the final expression for  $V$  in configuration space has to be completed by an overall factor  $\frac{g^4}{16\sqrt{2}\pi^2}$ ):

$$\begin{aligned} & \int d^2\boldsymbol{\rho}_1 d^2\boldsymbol{\rho}_2 \Phi_4(\boldsymbol{\rho}_1, \boldsymbol{\rho}_1, \boldsymbol{\rho}_1, \boldsymbol{\rho}_2) \frac{1}{2} \delta^{(2)}(\boldsymbol{\rho}_{12}) (\nabla_1 + \nabla_2)^2 \Phi_2(\boldsymbol{\rho}_1, \boldsymbol{\rho}_2) \\ & + \frac{1}{2\pi} \int d^2\boldsymbol{\rho}_1 d^2\boldsymbol{\rho}_2 \nabla_1^2 \Phi_4(\boldsymbol{\rho}_1, \boldsymbol{\rho}_1, \boldsymbol{\rho}_1, \boldsymbol{\rho}_2) \left[ \ln \frac{2}{|\boldsymbol{\rho}_{12}|} - \ln \lambda + \psi(1) \right] \nabla_2^2 \Phi_2(\boldsymbol{\rho}_1, \boldsymbol{\rho}_2) \\ & + \int d^2\boldsymbol{\rho}_1 d^2\boldsymbol{\rho}_2 d^2\boldsymbol{\rho}_0 \Phi_4(\boldsymbol{\rho}_1, \boldsymbol{\rho}_1, \boldsymbol{\rho}_1, \boldsymbol{\rho}_2) \frac{1}{(2\pi)^2} \left( \frac{\theta(|\boldsymbol{\rho}_{10}| - \epsilon)}{|\boldsymbol{\rho}_{10}|^2} + c(\epsilon, \lambda) \delta^{(2)}(\boldsymbol{\rho}_{10}) \right) \nabla_0^2 \nabla_2^2 \Phi_2(\boldsymbol{\rho}_0, \boldsymbol{\rho}_2) \end{aligned} \quad (4.1)$$

with  $c(\epsilon, \lambda)$  from (13). One sees that the constant pieces  $\ln 2 - \ln \lambda + \psi(1)$  cancel, and we are left with:

$$\begin{aligned} & \int d^2\boldsymbol{\rho}_1 d^2\boldsymbol{\rho}_2 \Phi_4(\boldsymbol{\rho}_1, \boldsymbol{\rho}_1, \boldsymbol{\rho}_1, \boldsymbol{\rho}_2) \frac{1}{2} \delta^{(2)}(\boldsymbol{\rho}_{12}) (\nabla_1 + \nabla_2)^2 \Phi_2(\boldsymbol{\rho}_1, \boldsymbol{\rho}_2) \\ & - \frac{1}{2\pi} \int d^2\boldsymbol{\rho}_1 d^2\boldsymbol{\rho}_2 \nabla_1^2 \Phi_4(\boldsymbol{\rho}_1, \boldsymbol{\rho}_1, \boldsymbol{\rho}_1, \boldsymbol{\rho}_2) \ln |\boldsymbol{\rho}_{12}| \nabla_2^2 \Phi_2(\boldsymbol{\rho}_1, \boldsymbol{\rho}_2) \\ & + \frac{1}{(2\pi)^2} \int d^2\boldsymbol{\rho}_1 d^2\boldsymbol{\rho}_2 d^2\boldsymbol{\rho}_0 \Phi_4(\boldsymbol{\rho}_1, \boldsymbol{\rho}_1, \boldsymbol{\rho}_1, \boldsymbol{\rho}_2) \left( \frac{\theta(|\boldsymbol{\rho}_{10}| - \epsilon)}{|\boldsymbol{\rho}_{10}|^2} + 2\pi \delta^{(2)}(\boldsymbol{\rho}_{10}) \ln \epsilon \right) \nabla_0^2 \nabla_2^2 \Phi_2(\boldsymbol{\rho}_0, \boldsymbol{\rho}_2) . \end{aligned} \quad (4.2)$$

Before we apply the transformation of inversion, it will be convenient to perform a few changes. First we change the second term. After partial integration we get (cf. eq.(2.28)):

$$\begin{aligned} \nabla_1^2 \ln |\boldsymbol{\rho}_{12}| \Phi_2(\boldsymbol{\rho}_1, \boldsymbol{\rho}_2) &= \nabla_1 \left( \frac{\boldsymbol{\rho}_{12}}{|\boldsymbol{\rho}_{12}|^2} \Phi_2(\boldsymbol{\rho}_1, \boldsymbol{\rho}_2) + \ln |\boldsymbol{\rho}_{12}| \nabla_1 \Phi_2(\boldsymbol{\rho}_1, \boldsymbol{\rho}_2) \right) \\ &= 2\pi \delta^{(2)}(\boldsymbol{\rho}_{12}) \Phi_2(\boldsymbol{\rho}_1, \boldsymbol{\rho}_2) + 2 \frac{\boldsymbol{\rho}_{12}}{|\boldsymbol{\rho}_{12}|^2} \nabla_1 \Phi_2(\boldsymbol{\rho}_1, \boldsymbol{\rho}_2) + \ln |\boldsymbol{\rho}_{12}| \nabla_1^2 \Phi_2(\boldsymbol{\rho}_1, \boldsymbol{\rho}_2) . \end{aligned} \quad (4.3)$$

Here the first term can be combined with the first term in (4.2). In the third term of (4.2) we split the  $\nabla_0^2$  operator: by partial integration we obtain:

$$\frac{1}{(2\pi)^2} \int d^2\boldsymbol{\rho}_1 d^2\boldsymbol{\rho}_2 d^2\boldsymbol{\rho}_0 \Phi_4(\boldsymbol{\rho}_1, \boldsymbol{\rho}_1, \boldsymbol{\rho}_1, \boldsymbol{\rho}_2) \left( \nabla_1 \frac{\theta(|\boldsymbol{\rho}_{10}| - \epsilon)}{|\boldsymbol{\rho}_{10}|^2} \nabla_0 + 2\pi \delta^{(2)}(\boldsymbol{\rho}_{10}) \ln \epsilon \nabla_0^2 \right) \nabla_2^2 \Phi_2(\boldsymbol{\rho}_0, \boldsymbol{\rho}_2) \quad (4.4)$$

We rescale the argument of the  $\theta$ -function and obtain the additional logarithm  $2\pi \ln |\boldsymbol{\rho}_{12}|$ . After differentiation we arrive at:

$$\begin{aligned} & \frac{1}{(2\pi)^2} \int d^2\boldsymbol{\rho}_1 d^2\boldsymbol{\rho}_2 d^2\boldsymbol{\rho}_0 \Phi_4(\boldsymbol{\rho}_1, \boldsymbol{\rho}_1, \boldsymbol{\rho}_1, \boldsymbol{\rho}_2) \left( \nabla_1 \frac{\theta(\frac{|\boldsymbol{\rho}_{10}|}{|\boldsymbol{\rho}_{12}|} - \epsilon)}{|\boldsymbol{\rho}_{10}|^2} \nabla_0 + 2\pi \delta^{(2)}(\boldsymbol{\rho}_{10}) \ln \epsilon \nabla_0^2 \right) \nabla_2^2 \Phi_2(\boldsymbol{\rho}_0, \boldsymbol{\rho}_2) \\ & + \frac{1}{2\pi} \int d^2\boldsymbol{\rho}_1 d^2\boldsymbol{\rho}_2 d^2\boldsymbol{\rho}_0 \Phi_4(\boldsymbol{\rho}_1, \boldsymbol{\rho}_1, \boldsymbol{\rho}_1, \boldsymbol{\rho}_2) \left( \frac{\boldsymbol{\rho}_{12} \nabla_1}{|\boldsymbol{\rho}_{12}|^2} + \ln |\boldsymbol{\rho}_{12}| \nabla_1^2 \right) \nabla_2^2 \Phi_2(\boldsymbol{\rho}_1, \boldsymbol{\rho}_2) . \end{aligned} \quad (4.5)$$

The next-to-last term combines with a similar term in (4.3), the last term cancels against the third piece of (4.3). Eq.(4.2) therefore takes the form:

$$\begin{aligned} & \int d^2\boldsymbol{\rho}_1 d^2\boldsymbol{\rho}_2 \Phi_4(\boldsymbol{\rho}_1, \boldsymbol{\rho}_1, \boldsymbol{\rho}_1, \boldsymbol{\rho}_2) \left( \delta^{(2)}(\boldsymbol{\rho}_{12}) \nabla_1 \nabla_2 - \frac{1}{2\pi} \frac{\boldsymbol{\rho}_{12}}{|\boldsymbol{\rho}_{12}|^2} \nabla_1 \nabla_2^2 \right) \Phi_2 f(\boldsymbol{\rho}_1, \boldsymbol{\rho}_2) \\ & + \frac{1}{(2\pi)^2} \int d^2\boldsymbol{\rho}_1 d^2\boldsymbol{\rho}_2 d^2\boldsymbol{\rho}_0 \Phi_4(\boldsymbol{\rho}_1, \boldsymbol{\rho}_1, \boldsymbol{\rho}_1, \boldsymbol{\rho}_2) \cdot \\ & \cdot \left( \nabla_1 \frac{\theta(\frac{|\boldsymbol{\rho}_{10}|}{|\boldsymbol{\rho}_{12}|} - \epsilon)}{|\boldsymbol{\rho}_{10}|^2} \nabla_0 + 2\pi \delta^{(2)}(\boldsymbol{\rho}_{10}) \ln \epsilon \nabla_0^2 \right) \nabla_2^2 \Phi_2(\boldsymbol{\rho}_0, \boldsymbol{\rho}_2) . \end{aligned} \quad (4.6)$$

As in the case of the BFKL kernel it will now be convenient to switch to the complex notation. With  $\nabla^2 = 4\partial\partial^*$  eq.(4.6) becomes:

$$\begin{aligned}
& 4 \int d^2\boldsymbol{\rho}_1 d^2\boldsymbol{\rho}_2 \Phi_4(\boldsymbol{\rho}_1, \boldsymbol{\rho}_1, \boldsymbol{\rho}_1, \boldsymbol{\rho}_2) \left( \frac{1}{2} \delta^{(2)}(\boldsymbol{\rho}_{12}) (\partial_1 \partial_2^* + \partial_1^* \partial_2) - \frac{1}{2\pi} \left( \frac{1}{\rho_{12}} \partial_1^* + \text{h.c.} \right) |\partial_2|^2 \right) \Phi_2(\boldsymbol{\rho}_1, \boldsymbol{\rho}_2) \\
& + \frac{2}{\pi^2} \int d^2\boldsymbol{\rho}_1 d^2\boldsymbol{\rho}_2 d^2\boldsymbol{\rho}_0 \Phi_4(\boldsymbol{\rho}_1, \boldsymbol{\rho}_1, \boldsymbol{\rho}_1, \boldsymbol{\rho}_2) \cdot \\
& \cdot \left( \partial_1 \frac{\theta(\frac{|\rho_{10}|}{|\rho_{12}|} - \epsilon)}{|\rho_{10}|^2} \partial_0^* + \text{h.c.} + 4\pi \delta^{(2)}(\boldsymbol{\rho}_{10}) \ln \epsilon |\partial_0|^2 \right) |\partial_2|^2 \Phi_2(\boldsymbol{\rho}_0, \boldsymbol{\rho}_2) .
\end{aligned} \tag{4.7}$$

This represents the configuration space expression for the first term of the group C.

Under the inversion transformation  $\rho \rightarrow 1/\rho$ ,  $\rho^* \rightarrow 1/\rho^*$  with

$$\delta^{(2)}(\boldsymbol{\rho}_{12}) \rightarrow |\rho_1|^2 |\rho_2|^2 \delta^{(2)}(\boldsymbol{\rho}_{12}) \tag{4.8}$$

eq.(4.3) turns into:

$$\begin{aligned}
& 4 \int d^2\boldsymbol{\rho}_1 d^2\boldsymbol{\rho}_2 \Phi_4(\boldsymbol{\rho}_1, \boldsymbol{\rho}_1, \boldsymbol{\rho}_1, \boldsymbol{\rho}_2) \left( \frac{1}{2} \delta^{(2)}(\boldsymbol{\rho}_{12}) (\partial_1 \partial_2^* + \partial_1^* \partial_2) - \frac{1}{2\pi} \left( \frac{\rho_2}{\rho_{12}\rho_1} \partial_1^* + \text{h.c.} \right) |\partial_2|^2 \right) \Phi_2(\boldsymbol{\rho}_1, \boldsymbol{\rho}_2) \\
& + \frac{2}{\pi^2} \int d^2\boldsymbol{\rho}_1 d^2\boldsymbol{\rho}_2 d^2\boldsymbol{\rho}_0 \Phi_4(\boldsymbol{\rho}_1, \boldsymbol{\rho}_1, \boldsymbol{\rho}_1, \boldsymbol{\rho}_2) \cdot \\
& \cdot \left( \partial_1 \frac{\theta(\frac{|\rho_{10}||\rho_1||\rho_2|}{|\rho_{12}||\rho_0|^2} - \epsilon)}{|\rho_{10}|^2} \frac{\rho_0^* \rho_1}{\rho_0 \rho_1^*} \partial_0^* + \text{h.c.} + 4\pi \delta^{(2)}(\boldsymbol{\rho}_{10}) \ln \epsilon |\partial_0|^2 \right) |\partial_2|^2 \Phi_2(\boldsymbol{\rho}_0, \boldsymbol{\rho}_2) .
\end{aligned} \tag{4.9}$$

In the second line we write:

$$\begin{aligned}
\frac{\rho_0^* \rho_1}{|\rho_{10}|^2 \rho_0 \rho_1^*} &= \frac{(\rho_{10} + \rho_0)(\rho_1 - \rho_{10})^*}{|\rho_{10}|^2 \rho_1^* \rho_0} \\
&= -\frac{1}{\rho_1^* \rho_0} + \frac{1}{\rho_{10}^* \rho_0} - \frac{1}{\rho_{10} \rho_1^*} + \frac{1}{|\rho_{10}|^2} .
\end{aligned} \tag{4.10}$$

In the first three terms the  $\theta$ -function can be ignored since the logarithmic divergence has disappeared. In the first term we make use of (2.29) and (2.30) and do the  $\rho_0$  integral via partial integration:

$$\int d^2\boldsymbol{\rho}_0 \left[ -\partial_1 \frac{1}{\rho_1^* \rho_0} \partial_0^* + \text{h.c.} \right] |\partial_2|^2 \Phi_2(\boldsymbol{\rho}_0, \boldsymbol{\rho}_2) = 2\pi^2 \delta^{(2)}(\boldsymbol{\rho}_1) |\partial_2|^2 \Phi_2(0, \boldsymbol{\rho}_2). \tag{4.11}$$

Similarly the second and the third term lead to:

$$\pi \left[ \frac{1}{\rho_1} \partial_1^* + \text{h.c.} \right] |\partial_2|^2 \Phi_2(\boldsymbol{\rho}_1, \boldsymbol{\rho}_2) \tag{4.12}$$

and

$$-2\pi^2 \delta^{(2)}(\boldsymbol{\rho}_1) |\partial_2|^2 \Phi_2(\boldsymbol{\rho}_1, \boldsymbol{\rho}_2) - \pi \left[ \frac{1}{\rho_1^*} \partial_1^* + \text{h.c.} \right] |\partial_2|^2 \Phi_2(\boldsymbol{\rho}_1, \boldsymbol{\rho}_2), \tag{4.13}$$

resp.. One easily sees that the first piece in (4.13) cancels against (4.11), the second piece in (4.13) against (4.12). So all we are left with is the fourth term in (4.10). Here we again rescale the argument of the  $\theta$  function, in order to compare with our starting expression (4.7). The additional logarithmic term has the form:

$$\begin{aligned} & \frac{4}{\pi} \int d^2 \boldsymbol{\rho}_1 d^2 \boldsymbol{\rho}_2 d^2 \boldsymbol{\rho}_0 \Phi_4(\boldsymbol{\rho}_1, \boldsymbol{\rho}_1, \boldsymbol{\rho}_1, \boldsymbol{\rho}_2) \left[ \partial_1 \ln \frac{|\rho_2|}{|\rho_1|} \partial_1^* + \text{h.c.} \right] |\partial_2|^2 \Phi_2(\boldsymbol{\rho}_1, \boldsymbol{\rho}_2) \\ &= \frac{4}{\pi} \int d^2 \boldsymbol{\rho}_1 d^2 \boldsymbol{\rho}_2 d^2 \boldsymbol{\rho}_0 \Phi_4(\boldsymbol{\rho}_1, \boldsymbol{\rho}_1, \boldsymbol{\rho}_1, \boldsymbol{\rho}_2) \left[ -\frac{1}{\rho_1} \partial_1^* - \text{h.c.} + 2 \ln \frac{|\rho_2|}{|\rho_1|} |\partial_1|^2 \right] |\partial_2|^2 \Phi_2(\boldsymbol{\rho}_1, \boldsymbol{\rho}_2) . \end{aligned} \quad (4.14)$$

Finally, in the first line of (4.9) we put

$$\frac{\rho_2}{\rho_{12}\rho_1} = \frac{1}{\rho_{12}} - \frac{1}{\rho_1}. \quad (4.15)$$

and observe that the second term cancels against the first part of the second line of (4.14). As a result of the inversion, we arrive at our old result plus the extra term:

$$\frac{8}{\pi} \int d^2 \boldsymbol{\rho}_1 d^2 \boldsymbol{\rho}_2 \Phi(\boldsymbol{\rho}_1, \boldsymbol{\rho}_1, \boldsymbol{\rho}_1, \boldsymbol{\rho}_2) \ln \frac{|\rho_2|}{|\rho_1|} |\partial_1|^2 |\partial_2|^2 \Phi_2(\boldsymbol{\rho}_1, \boldsymbol{\rho}_2). \quad (4.16)$$

Later on we shall see that this term will be cancelled by similar terms from A and B.

Next we turn to group A and consider the momentum set (1234). In configuration space we have:

$$\begin{aligned} & \int d^2 \boldsymbol{\rho}_1 d^2 \boldsymbol{\rho}_2 d^2 \boldsymbol{\rho}_0 \Phi_4(\boldsymbol{\rho}_1, \boldsymbol{\rho}_0, \boldsymbol{\rho}_0, \boldsymbol{\rho}_2) \nabla_0^2 \frac{\ln |\rho_{10}| \ln |\rho_{20}|}{(2\pi)^2} \nabla_1^2 \nabla_2^2 \Phi_2(\boldsymbol{\rho}_1, \boldsymbol{\rho}_2) \\ & - \frac{1}{(2\pi)^2} \int d^2 \boldsymbol{\rho}_1 d^2 \boldsymbol{\rho}_2 d^2 \boldsymbol{\rho}_0 \Phi_4(\boldsymbol{\rho}_1, \boldsymbol{\rho}_1, \boldsymbol{\rho}_1, \boldsymbol{\rho}_2) \left( \frac{\theta(|\rho_{10}| - \epsilon)}{|\rho_{10}|^2} + 2\pi \delta^{(2)}(\boldsymbol{\rho}_{10}) \ln \epsilon \right) \nabla_1^2 \nabla_2^2 \Phi_2(\boldsymbol{\rho}_1, \boldsymbol{\rho}_2) \\ & - \frac{1}{(2\pi)^2} \int d^2 \boldsymbol{\rho}_1 d^2 \boldsymbol{\rho}_2 d^2 \boldsymbol{\rho}_0 \Phi_4(\boldsymbol{\rho}_1, \boldsymbol{\rho}_2, \boldsymbol{\rho}_2, \boldsymbol{\rho}_2) \left( \frac{\theta(|\rho_{20}| - \epsilon)}{|\rho_{20}|^2} + 2\pi \delta^{(2)}(\boldsymbol{\rho}_{20}) \ln \epsilon \right) \nabla_1^2 \nabla_2^2 \Phi_2(\boldsymbol{\rho}_1, \boldsymbol{\rho}_2) . \end{aligned} \quad (4.17)$$

Here we have already omitted the constant pieces  $\ln 2 - \ln \lambda + \psi(1)$ : they appear both in the first line (in combination with  $\ln |\rho_{10}|$ ) and the trajectory function term in the second and third term, and in the sum they cancel. In the first term we take the derivative with respect to  $\rho_0$ :

$$\nabla_0^2 \ln |\rho_{10}| \ln |\rho_{20}| = 2\pi \delta^{(2)}(\boldsymbol{\rho}_{10}) \ln |\rho_{20}| + 2\pi \delta^{(2)}(\boldsymbol{\rho}_{20}) \ln |\rho_{10}| + 2 \frac{\boldsymbol{\rho}_{10} \cdot \boldsymbol{\rho}_{20}}{|\rho_{10}|^2 |\rho_{20}|^2}. \quad (4.18)$$

In the first two terms we use the  $\delta$ -functions and perform the  $\rho_0$  integral. The third term can be combined with the  $\theta$ -function pieces in (4.17) which we rewrite in a symmetric form  $\theta(|\rho_{10}| - \epsilon) = \theta(\frac{|\rho_{10}||\rho_{20}|}{|\rho_{12}|} - \epsilon)$ . The result is:

$$\begin{aligned} & \frac{1}{(2\pi)} \int d^2 \boldsymbol{\rho}_1 d^2 \boldsymbol{\rho}_2 (\Phi_4(\boldsymbol{\rho}_1, \boldsymbol{\rho}_1, \boldsymbol{\rho}_1, \boldsymbol{\rho}_2) \ln |\rho_{12}| + \Phi_4(\boldsymbol{\rho}_1, \boldsymbol{\rho}_2, \boldsymbol{\rho}_2, \boldsymbol{\rho}_2) \ln |\rho_{12}|) \\ & - \frac{1}{(2\pi)^2} \int d^2 \boldsymbol{\rho}_1 d^2 \boldsymbol{\rho}_2 d^2 \boldsymbol{\rho}_0 \Phi_4(\boldsymbol{\rho}_1, \boldsymbol{\rho}_0, \boldsymbol{\rho}_0, \boldsymbol{\rho}_2) \cdot \\ & \cdot \left( \frac{|\rho_{12}|^2}{|\rho_{10}|^2 |\rho_{20}|^2} \theta\left(\frac{|\rho_{10}||\rho_{20}|}{|\rho_{12}|} - \epsilon\right) + 2\pi \ln \epsilon \left[ \delta^{(2)}(\boldsymbol{\rho}_{10}) + \delta^{(2)}(\boldsymbol{\rho}_{20}) \right] \right) \nabla_1^2 \nabla_2^2 \Phi_2(\boldsymbol{\rho}_1, \boldsymbol{\rho}_2) . \end{aligned} \quad (4.19)$$

The first line can be absorbed into the  $\theta$ -functions (cf. (2.21)). So we are left with:

$$- \frac{1}{(2\pi)^2} \int d^2 \rho_1 d^2 \rho_2 d^2 \rho_0 \Phi_4(\rho_1, \rho_0, \rho_0, \rho_2) \cdot \left( \frac{|\rho_{12}|^2}{|\rho_{10}|^2 |\rho_{20}|^2} \theta\left(\frac{|\rho_{10}| |\rho_{20}|}{|\rho_{12}|^2} - \epsilon\right) + 2\pi \ln \epsilon \left[ \delta^{(2)}(\rho_{10}) + \delta^{(2)}(\rho_{20}) \right] \right) \nabla_1^2 \nabla_2^2 \Phi_2(\rho_1, \rho_2) \cdot \quad (4.20)$$

We again switch to the complex notation:

$$- \frac{4}{\pi^2} \int d^2 \rho_1 d^2 \rho_2 d^2 \rho_0 \Phi_4(\rho_1, \rho_0, \rho_0, \rho_2) \cdot \left( \frac{|\rho_{12}|^2}{|\rho_{10}|^2 |\rho_{20}|^2} \theta\left(\frac{|\rho_{10}| |\rho_{20}|}{|\rho_{12}|^2} - \epsilon\right) + 2\pi \ln \epsilon \left[ \delta^{(2)}(\rho_{10}) + \delta^{(2)}(\rho_{20}) \right] \right) |\partial_1|^2 |\partial_2|^2 \Phi_2(\rho_1, \rho_2) \cdot \quad (4.21)$$

This is the configuration space expression of the first term in A.

Under the inversion only the  $\theta$ -function requires a little calculation. Its argument behaves as:

$$\frac{|\rho_{10}| |\rho_{20}|}{|\rho_{12}|^2} \rightarrow \frac{|\rho_{10}| |\rho_{20}|}{|\rho_{12}|^2} \frac{|\rho_1| |\rho_2|}{|\rho_0|^2}, \quad (4.22)$$

which is equivalent to having the extra term

$$- \frac{8}{\pi} \int d^2 \rho_1 d^2 \rho_2 \left( \Phi_4(\rho_1, \rho_1, \rho_1, \rho_2) \ln \frac{|\rho_2|}{|\rho_1|} + \Phi_4(\rho_1, \rho_2, \rho_2, \rho_2) \ln \frac{|\rho_1|}{|\rho_2|} \right) |\partial_1|^2 |\partial_2|^2 \Phi_2(\rho_1, \rho_2). \quad (4.23)$$

Finally we come to group B (first line in Fig.4, momenta (1234)). It differs from A by the overall sign and the arguments of  $\Phi_4$  which are replaced by  $\Phi_4(\rho_1, \rho_1, \rho_0, \rho_2)$ . Repeating the same sequence of steps we find that, under inversion, the additional terms analogous to (4.23) are:

$$\frac{8}{\pi} \int d^2 \rho_1 d^2 \rho_2 \left( \Phi_4(\rho_1, \rho_1, \rho_1, \rho_2) \ln \frac{|\rho_2|}{|\rho_1|} + \Phi_4(\rho_1, \rho_1, \rho_2, \rho_2) \ln \frac{|\rho_1|}{|\rho_2|} \right) |\partial_1|^2 |\partial_2|^2 \Phi_2(\rho_1, \rho_2). \quad (4.24)$$

One notices that the remainders of A, B, and C (in (4.23), (4.24), and (4.16), respectively) are all of the same form but differ in the arguments of  $\Phi_4$ . As a final step, we have to include the permutations of the arguments, as indicated in Fig.4. In an obvious notation, we have:

$$\begin{aligned} A : & [1234] + [2134] + [1243] + [2143] \\ B : & [1234] + [1243] + \text{second line} \\ C : & [1234] + [1243] + \text{second line}. \end{aligned} \quad (4.25)$$

Inserting these changes of arguments into (4.23) we obtain for A:

$$- \frac{16}{\pi} \int d^2 \rho_1 d^2 \rho_2 \left( [\Phi_4(\rho_1, \rho_1, \rho_1, \rho_2) + \Phi_4(\rho_1, \rho_1, \rho_2, \rho_1)] \ln \frac{|\rho_2|}{|\rho_1|} + [\Phi_4(\rho_1, \rho_2, \rho_2, \rho_2) + \Phi_4(\rho_2, \rho_1, \rho_2, \rho_2)] \ln \frac{|\rho_1|}{|\rho_2|} \right) |\partial_1|^2 |\partial_2|^2 \Phi_2(\rho_1, \rho_2) \cdot \quad (4.26)$$

Similarly for B in (4.24):

$$\begin{aligned} & \frac{8}{\pi} \int d^2 \rho_1 d^2 \rho_2 \left( [\Phi_4(\rho_1, \rho_1, \rho_1, \rho_2) + \Phi_4(\rho_1, \rho_1, \rho_2, \rho_1) + 2\Phi_4(\rho_1, \rho_1, \rho_2, \rho_2)] \ln \frac{|\rho_2|}{|\rho_1|} \right. \\ & \left. + [2\Phi_4(\rho_1, \rho_1, \rho_2, \rho_2) + \Phi_4(\rho_1, \rho_2, \rho_2, \rho_2) + \Phi_4(\rho_2, \rho_1, \rho_2, \rho_2)] \ln \frac{|\rho_1|}{|\rho_2|} \right) |\partial_1|^2 |\partial_2|^2 \Phi_2(\rho_1, \rho_2) . \end{aligned} \quad (4.27)$$

In the same way we find for the remainders of C in (4.16):

$$\begin{aligned} & \frac{8}{\pi} \int d^2 \rho_1 d^2 \rho_2 \left( [\Phi_4(\rho_1, \rho_1, \rho_1, \rho_2) + \Phi_4(\rho_1, \rho_1, \rho_2, \rho_1)] \ln \frac{|\rho_2|}{|\rho_1|} \right. \\ & \left. + [\Phi_4(\rho_1, \rho_2, \rho_2, \rho_2) + \Phi_4(\rho_2, \rho_1, \rho_2, \rho_2)] \ln \frac{|\rho_1|}{|\rho_2|} \right) |\partial_1|^2 |\partial_2|^2 \Phi_2(\rho_1, \rho_2) . \end{aligned} \quad (4.28)$$

Taking the sum of (4.26) and (4.27) and (4.28), we arrive at zero. This completes our proof that the sum of the terms A, B, C is invariant under the inversion of coordinates. As it was said before, the last group D has the form of the BFKL kernel and is therefore invariant by itself.

## 5 Conclusions

The result of this paper is the invariance of the effective  $2 \rightarrow 4$  gluon vertex under Möbius transformations, in particular the inversion  $\rho \rightarrow 1/\rho$ . As a consequence, one expects that the quantum mechanical problem of  $n$  pairwise-interacting gluons which due to the existence of the number non-conserving vertex now turns into a quantum field theory preserves the conformal invariance. As the next step it is extremely important to find out whether the transition vertex is separable, i.e. it can be written as a sum of two terms which depend only upon either the  $\rho$ 's or the  $\rho^*$ 's. It is, therefore, very desirable to find a compact form in analogy to (1.1) - (1.4). Work in this direction is in progress.

**Acknowledgements:** One of us (L.L.) wishes to thank DESY and the II.Institut für Theoretische Physik, Universität Hamburg, for their hospitality and the Alexander von Humboldt Foundation for the financial support. We thank H.Lotter for helpful discussions on the proof of conformal invariance of the BFKL kernel.

## References

- [1] E.A.Kuraev and L.N.Lipatov,V.S.Fadin, *Sov.Phys.JETP* **44** (1976) 443,  
*Sov.Phys.JETP* **45** (1977) 199,  
Y.Y.Balitskij and L.N.Lipatov, *Sov.J.Nucl.Phys* **28** (1978) 822.
- [2] L.N.Lipatov, *Sov.Phys.JETP* **63** (1986) 904.
- [3] L.N.Lipatov, *Phys.Lett.* **B309** (1993) 394.
- [4] J.Bartels, *Nucl.Phys.* **B175** (1980) 365,  
J.Kwiecinski, M.Praszalowicz, *Phys.Lett.* **B94** (1980) 413.
- [5] L.N.Lipatov, *JETP Lett.* **59** (1994) 596.
- [6] L.D.Faddeev, G.P.Korchemsky, *Phys.Lett* **B342** (1995) 311.
- [7] J.Bartels, *Z.Phys.* **C60** (1993) 471, *Phys.Lett.* **B298** (1993) 204.
- [8] J.Bartels, M.Wüsthoff, *Z.Phys.* **C66** (1995) 157.
- [9] V.S.Fadin, R.Fiore, A.Quartarolo, preprint BUDKERINP-95-49, *Phys.Rev.* **D50** (1994) 5893,  
*Phys.Rev.* **D50** (1994) 2265,  
V.S.Fadin, L.N.Lipatov *Nucl.Phys.* **B406** (1993) 259,  
V.S.Fadin, R.Fiore, *Phys.Lett.* **B294** (1992) 286,  
V.S.Fadin, L.N.Lipatov *JETP Lett.* **49** (1989) 352, *Sov.J.Nucl.Phys.* **50** (1989) 712.
- [10] R.K.Ellis, Z.Kunszt, E.M.Levin, *Nucl.Phys.* **B420** (1994) 517-549,  
ERRATUM-ibid. **B433** (1995) 498.
- [11] R.K.Ellis, F.Hautmann, B.R.Webber, *Phys.Lett.* **B348** (1995) 582.
- [12] R.D. Ball, S.Forte, *Phys.Lett.* **B351** (1995) 313.
- [13] L.N.Lipatov, preprint DESY-95-029.
- [14] L.N.Lipatov, *Nucl.Phys.* **B365** (1991) 614.
- [15] P.Gauron, L.N.Lipatov, B.Niculescu, *Phys.Lett.* **B260** (1991) 407; *Phys.Lett.* **B304** (1993) 334.

## Figure captions

**Fig.1:** The BFKL equation (2.6).

**Fig.2:** The structure of the BFKL kernel

(a) real production in the BFKL kernel; (b) the effective BFKL kernel.

**Fig.3:** The structure of the  $2 \rightarrow 4$  transition kernel

(a) real production which leads to a connected contribution; (b) real production which gives a disconnected contribution; (c) reggeization and the  $2 \rightarrow 3$  transition vertex. The dashed line denotes the s-channel cutting. (d) structure of the full  $2 \rightarrow 4$  transition vertex (shown are the contributions from (a) and (c)).

**Fig.4:** The complete representation of the  $2 \rightarrow 4$  transition vertex.

**Fig.5:** The transition vertex combined with the non-amputated amplitudes for 2 and 4 gluons,  $\Phi_2$  and  $\Phi_4$ .

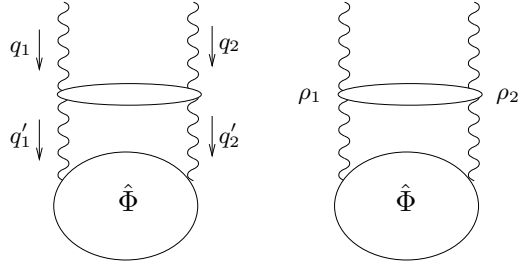
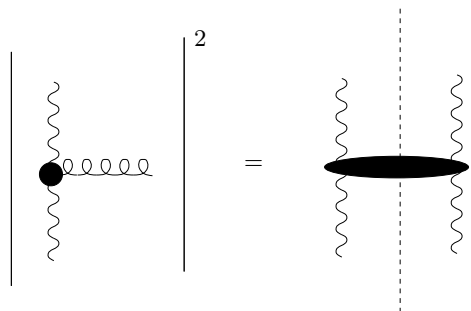
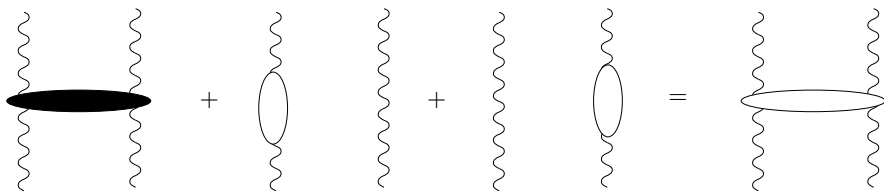


Figure 1:

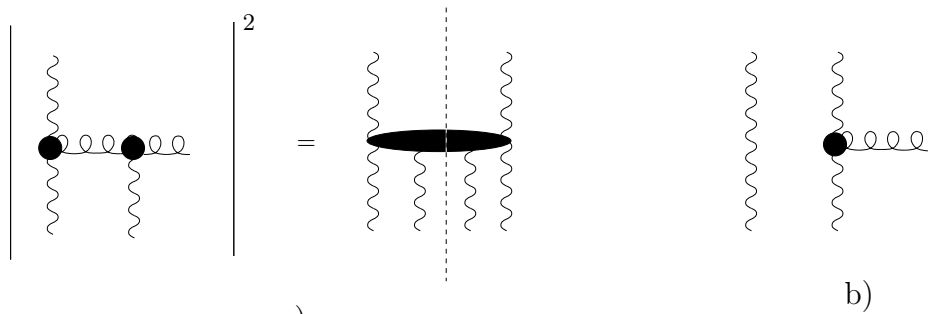


a)

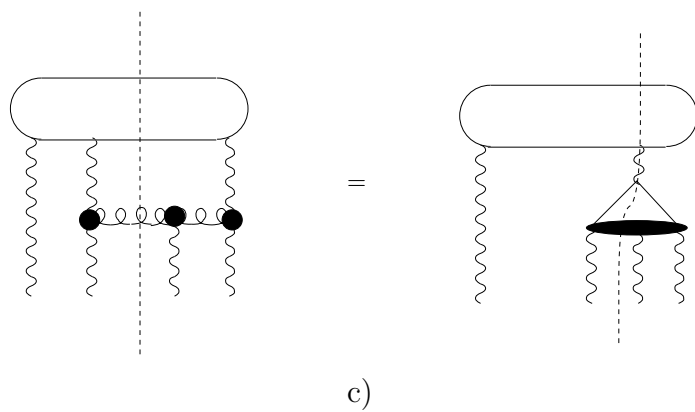


b)

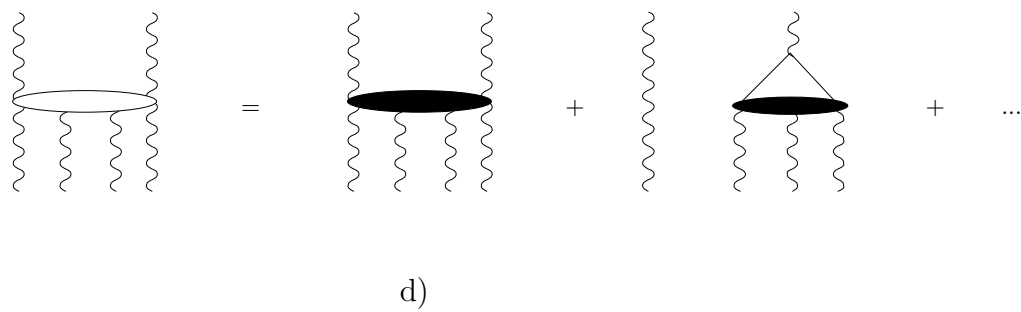
Figure 2:

a) 

$$\left| \begin{array}{c} \text{Diagram with two vertices and four loops} \end{array} \right|^2 = \begin{array}{c} \text{Diagram with horizontal line and four wavy lines} \end{array} + \begin{array}{c} \text{Diagram with one vertex and four wavy lines} \end{array}$$

c) 

$$\begin{array}{c} \text{Diagram with horizontal line and four vertices} \end{array} = \begin{array}{c} \text{Diagram with horizontal line and four vertices, middle two connected by a triangle} \end{array}$$

d) 

$$\begin{array}{c} \text{Diagram with horizontal line and four wavy lines} \end{array} = \begin{array}{c} \text{Diagram with horizontal line and four wavy lines} \end{array} + \begin{array}{c} \text{Diagram with triangle and four wavy lines} \end{array} + \dots$$

Figure 3:

$$\begin{array}{c}
\left. \begin{array}{c}
- \quad \begin{array}{|c|} \hline \diagup \quad \diagdown \\ \hline \end{array} \quad + \frac{1}{2} \quad \begin{array}{|c|} \hline \diagup \quad \diagdown \\ \hline \end{array} \quad + \frac{1}{2} \quad \begin{array}{|c|} \hline \diagup \quad \diagdown \\ \hline \end{array} \\
[1234] + [2134] + [1243] + [2143]
\end{array} \right\} \mathbf{A}
\\[20pt]
\left. \begin{array}{c}
\begin{array}{|c|} \hline \diagup \quad \diagdown \\ \hline \end{array} \quad - \frac{1}{2} \quad \begin{array}{|c|} \hline \diagup \quad \diagdown \\ \hline \end{array} \quad - \frac{1}{2} \quad \begin{array}{|c|} \hline \diagup \quad \diagdown \\ \hline \end{array} \\
[1234] + [1243] \\
\begin{array}{|c|} \hline \diagup \quad \diagdown \\ \hline \end{array} \quad - \frac{1}{2} \quad \begin{array}{|c|} \hline \diagup \quad \diagdown \\ \hline \end{array} \quad - \frac{1}{2} \quad \begin{array}{|c|} \hline \diagup \quad \diagdown \\ \hline \end{array} \\
[1234] + [2134]
\end{array} \right\} \mathbf{B}
\\[20pt]
\left. \begin{array}{c}
\begin{array}{|c|} \hline \diagup \quad \diagdown \\ \hline \end{array} \quad - \frac{1}{2} \quad \begin{array}{|c|} \hline \diagup \quad \diagdown \\ \hline \end{array} \quad - \frac{1}{2} \quad \begin{array}{|c|} \hline \diagup \quad \diagdown \\ \hline \end{array} \\
[1234] + [1243] \\
\begin{array}{|c|} \hline \diagup \quad \diagdown \\ \hline \end{array} \quad - \frac{1}{2} \quad \begin{array}{|c|} \hline \diagup \quad \diagdown \\ \hline \end{array} \quad - \frac{1}{2} \quad \begin{array}{|c|} \hline \diagup \quad \diagdown \\ \hline \end{array} \\
[1234] + [2134]
\end{array} \right\} \mathbf{C}
\\[20pt]
\left. \begin{array}{c}
\begin{array}{|c|} \hline \diagup \quad \diagdown \\ \hline \end{array} - \begin{array}{|c|} \hline \diagup \quad \diagdown \\ \hline \end{array} - \begin{array}{|c|} \hline \diagup \quad \diagdown \\ \hline \end{array} + \frac{1}{2} \quad \begin{array}{|c|} \hline \diagup \quad \diagdown \\ \hline \end{array} + \frac{1}{2} \quad \begin{array}{|c|} \hline \diagup \quad \diagdown \\ \hline \end{array} \\
[1234]
\end{array} \right\} \mathbf{D}
\end{array}$$

Figure 4:

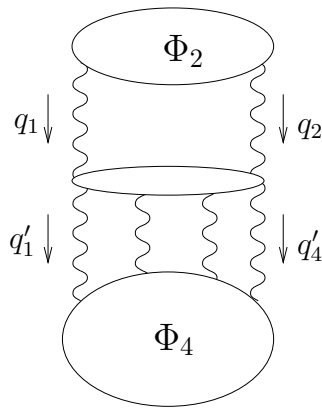


Figure 5: